NASA TECHNICAL MEMORANDUM

NASA TM X-52870

NASA TM X-52870

SPECTRAL RESPONSES OF SILICON SOLAR CELLS AT LOW TEMPERATURE

by Henry W. Brandhorst, Jr. and Russell E. Hart, Jr.
Lewis Research Center
Cleveland, Ohio

TECHNICAL PAPER proposed for presentation at
Eighth Photovoltaic Specialists Conference
Seattle, Washington, August 4-6, 1970

SPECTRAL RESPONSES OF SILICON SOLAR CELLS AT LOW TEMPERATURES

by Henry W. Brandhorst, Jr. and Russell E. Hart, Jr.

Lewis Research Center
National Aeronautics and Space Administration
Cleveland, Ohio

E-5837

SUMMARY

Spectral responses were measured at temperatures down to 95°K for silicon solar cells with poor and good performance at low temperatures. Poor cells had either a rectifying rear contact or a flat spot on the I-V curve and a rapid decrease in I_{SC} at low temperatures. Good cells showed a gradual loss in red response that was due to the change of absorption coefficient with temperature. A further loss in red response was responsible for the rapid decrease in current in poor cells. The flat spot and the loss in current appear to be related.

INTRODUCTION

Previous studies (1-5) have indicated wide variability in the performance of silicon solar cells at low temperatures and illumination intensities. At first (1,2), it was thought that only high cell leakage currents contributed to the poor low temperature performance. Later, however, other factors that lead to poor performance were observed (5). These include a Schottky barrier at the rear contact, the flat spot on the current-voltage (I-V) trace around the maximum power point and an abrupt loss in short circuit current at the lower temperatures. The reasons for and the solution to the Schottky barrier at the rear contact are straightforward. However, it is not clear why the latter two factors appear or if they are related or independent. It is hoped that an understanding of these factors will lead not only to an improved low temperature cell but also to improvements in cells for more conventional applications.

From the information available on the flat spot and the loss of short circuit current, it is not possible to tell whether the problems lie in the bulk region of the cell, in the junction itself or in the diffused layer. Spectral response measurements provide clues that help to isolate the region responsible for the effect. In general, losses in the red region of the spectral response suggest losses in the bulk region or the back contact, an overall decrease in response suggests junction problems and a loss of blue response can be indicative that the problem lies in the diffused region or the front contact. The purpose of the work described in this paper was to measure the spectral responses of selected cells at low temperatures in order to help determine the region of the cell responsible for the abrupt loss of short circuit current with decreasing temperature.

The cells used in this work were selected from those described in reference 5. One ion implanted cell and one diffused junction cell each showing good low temperature performance were selected. Also included was a cell with a Schottky barrier at the rear contact and a cell with a flat spot on the I-V curve and a simultaneous loss in short circuit current at low temperatures.

EXPERIMENTAL PROCEDURE

The cells used in this study were typical of those in current production and being supplied for spacecraft applications. The dimensions were 2 cm x 2 cm and were obtained from different manufacturers. Their room temperature performances are all similar. The apparatus and techniques used for measuring the performance curves of these cells was described previously (2,5).

Figure 1 shows the apparatus used for making the spectral response measurements. The cells were mounted on a liquid-nitrogen cooled test block in a small vacuum chamber. Temperature control was ±1°C (5) and chamber pressure was less than 10^{-3} torr. Monochromatic illumination was obtained using narrow bandpass interference filters mounted on an indexing table. Of the twenty available

(1) C. H. Liebert, "Solar Cell Performance at Jupiter Temperature and Solar Intensity," Presented at Seventh IEEE Photovoltaic Specialists Conference, Pasadena, Calif., Nov. 19-21, 1968.

(2) C. H. Liebert and R. E. Hart, Jr., "Solar-Cell Performance at Low Temperatues and Simulated Solar Intensities," NASA TN D-5547, 1969.

(3) R. J. Lambert, "Characteristics of Solar Cells at Low Temperatures," Conference Record of the Seventh Photovoltaic Specialists Conference, IEEE, pp. 97-100; 1968.

(4) E. L. Ralph, "Performance of Very Thin Silicon Solar Cells," Conference Record of the Sixth Photovoltaic Specialists Conference, Vol. 1, IEEE, pp. 98-116; 1967.

(5) H. W. Brandhorst, Jr. and R. E. Hart, Jr., "Effects of Decreasing Temperature and Illumination Intensity in Silicon Solar Cell Performance," NASA TM X-52756, 1970.

positions on the table, interference filters occupy eighteen. The interval from 0.5 to 1.1 μm is covered in 0.05 μm steps while the interval from 0.375 to 0.5 μm is covered in roughly 0.025 μm steps. The full bandwidth at half-maximum of the filters is less than 0.02 μ. The light source is a 1000 watt tungsten-iodine lamp with reflector, projecting through a 2" water filter. The water filter contains a recirculating 1 g/liter $CuSO_4$ solution. Light intensities of the tungsten-iodine lamp source is set with a standard silicon solar cell (6) located under a neutral density screen placed in one of the remaining positions on the filter array. The light intensity coming through the filters is measured before each run using a wide angle, sixteen junction, bismuth-silver thermopile. Output of the cell is measured across a one-ohm resistor using a high impedance digital voltmeter. Relative spectral responses were calculated by dividing the current output of the cell by the energy density (mw/cm^2) of the monochromatic beams.

RESULTS AND DISCUSSION

Performance Curves

Figures 2a and b and 3a and b show the performance curves of four silicon solar cells selected from those measured previously (5). For the sake of brevity, only the data at 4.6 mw/cm^2 are shown. Performance curves at 2.7, 4.6, 12, and 136 mw/cm^2 are shown in the earlier paper. These cells (IP6, C191, C206, and C214) were chosen because they exhibit the range of effects, from good to bad, that have been seen in the cells. Pertinent performance characteristics are listed in table 1.

Cells IP6 and C191 are good cells as indicated by the linearity of their V_{OC} and I_{SC} curves as a function of temperature. The efficiency curves are also basically linear showing only a slight curvature at the lower temperatures. Both cells showed a slight indication of a Schottky barrier at the rear contact at low temperatures, however. The presence of this barrier was indicated by a decrease in V_{OC} with increasing illumination intensity, and by a curvature of the I-V plot near the open circuit voltage point. In spite of this slight problem the efficiencies of these cells under near-Jupiter conditions (4.6 mw/cm^2 and 140°K) are high (15.3 and 15.6 percent respectively). Cell IP6 is included in this paper because it represents an ion-implanted junction whose behavior can be contrasted to the standard diffused junction cell.

The performance curves of C206 and C214 show abrupt decreases in short circuit current at about 180-200°K. The decrease for C214 is very slight however. Also, both cells show curvature of both the V_{OC} and efficiency curves with temperature.

Cell C206 had an exceedingly bad flat spot around the maximum power point as shown by figure 4. These four curves were measured at intensities of 2.7, 4.6, 12.0 and 136 mw/cm^2 at a temperature of 122°K. The flat spot is so bad that at the low intensities there is a loss in the open-circuit voltage because the flat spot crosses the voltage axis. The efficiency of this cell is only 9.1 percent under near-Jupiter conditions.

On the other hand, C214 had a strong Schottky barrier at the rear contact as shown in figure 5. This barrier is clearly identified by either the curvature of the I-V plot near the open circuit voltages or by the decrease in the V_{OC} with increasing light intensity. Only the two higher light intensities are shown as this most clearly shows the effect. It can be seen that at 136 mw/cm^2, the open-circuit voltage is about 0.1 volt less than the V_{OC} at 12 mw/cm^2.

Spectral Response Curves

The relative spectral response curves (uncorrected for reflection losses) of cells IP6 and C191 are shown in figure 6a and b. The temperature range covered is between 95 and 299°K. In general, there is an even loss of the red response of the cell. This is expected due to the increase in band gap of silicon and hence the decrease in the absorption coefficient at the red wavelength as the temperature is decreased. These cells showed only a gradual, constant loss of short circuit current with decreasing temperature. Spectral responses of cells C206 and C214 are shown in figure 7a and b. The results for C214 are similar to IP6 and C191; however, for C206, there appears an additional loss of red response. This cell showed a larger abrupt drop in short circuit current as the temperature decreased.

In order to show that indeed the measured spectral response accurately described the loss in short circuit current, the relative spectral response was multiplied both by Johnson's curve for air mass zero sunlight and by a typical spectrum from a solar simulator (although not the one used for the performance measurements). The product was normalized to the reading at 300°K. The results are compared to the measured values in figure 8 for a good cell, C191, and a bad cell, C206. It can be seen that the agreement is excellent. Similar fits were obtained for the other cells.

Response at Monochromatic Wavelengths

Response to 0.4 μm light. Figure 9 shows the responses of all four cells at 0.4 μm with decreasing temperature. Cell IP6 shows a steady decrease in output with decreasing temperature. Cells C191, C206 and C214, on the other hand, all show an increasing output with decreasing temperature. There is a slight drop in output for these three cells below about 130°K, however. This increase in 0.4 μm response as the temperature decreases has been seen on all diffused junction cells tested. It was somewhat unexpected, but is

(6) H. W. Brandhorst, Jr. and E. O. Boyer, "Calibration of Solar Cells Using High-Altitude Aircraft," NASA TN D-2508, 1965.

probably related to either an increase in diffusion length in the diffused layer or to a decreased surface recombination velocity.

Response to 1.0 μm light. As shown earlier, most of the characteristic changes in the spectral response curves occur in the red part of the spectrum. Figure 10 shows the responses of all cells to 1.0 μm light. The change in response at 1.0 μm can also be estimated from the variation of absorption coefficient of silicon with temperature (7). Because of a lack of detailed knowledge of the necessary parameters (8) of these cells in this work, no exact calculation of the response was attempted. Rather, a constant collection efficiency was assumed, and the number of photons absorbed was calculated as a function of decreasing temperature. These results were then normalized to the response at 300°K. These calculated points are shown as the shaded symbols on the curves.

For both cells IP6 and C191, excellent agreement is obtained. A slight difference appears below 100°K for cell IP6. The great difference in shape of the curves is due to the different thickness spread between IP6 and C191, excellent agreement is obtained. This confirms that the gradual, linear loss of short circuit current with temperature is caused by the increasing band gap of silicon.

The agreement between the calculated and observed data for cells C206 and C214 is not as good. Cell C214 (which had a Schottky barrier) shows reasonably good agreement down to about 200°K, where some deviation is noted. This discrepancy can be explained in terms of the Schottky barrier at the rear contact. This junction will also collect part of the current generated by the cell, albeit inefficiently. Those wavelengths of light (e.g., 1.0 μm) that penetrate deeply will generate electrons close enough to this junction to be collected. Additional experiments which confirmed that these barriers would collect the current were done on other cells. The collection of some of the electrons at the rear contact will cause a slight reduction in the 1.0 μm response of the cell but would probably not affect the overall short circuit current of the cell greatly. It can be seen that there is a very slight hop in the short circuit current of this cell beginning around 200°K (c.f. fig. 3b) that may be explained by this mechanism.

Cell C206 (which had the flat spot) shows a larger disagreement between calculated and experimental results. There appears to be an increasing spread between the results, the disagreement getting much worse below 180°K (the temperature at which the short circuit current begins to drop rapidly; c.f. fig. 3a). This additional loss of current may be caused by a loss in collected current (e.g. loss in diffusion length). It is not known what sort of collection losses are involved; however, the drastic loss of current shown throughout the red region of the response of this cell (c.f. fig. 7) suggests that a loss in diffusion length could be responsible. Additionally, recent work by Payne (9), has shown a difference between cells made from float zone refined and Czochralski grown ingots of silicon. The current loss at low temperatures in cells made from float zone material was less.

It is therefore possible that an oxygen impurity may be responsible for a reduction in diffusion length. At this time, however, this explanation must be considered to be tentative until other loss mechanisms, including cell contamination, are thoroughly examined.

Correlation Between Flat Spot and Current Loss

One of the curious features of the flat spot phenomenon is that the appearance of the flat spot coincides with the drop in short circuit current of the cell. For the four cells in reference 5 that showed both the flat spot and the loss of short circuit current, both effects appeared simultaneously at temperatures between about 180 and 220°K. This strongly suggests that both features are tied together and that a single mechanism will explain both these effects.

CONCLUSION

The gradual, linear decrease of the short circuit current of good silicon solar cells as the temperature is decreased is due to an increase in the band gap of silicon. This increasing band gap leads to a decreasing absorption coefficient especially at the long wavelengths. Accordingly, these cells showed a gradual, constant loss of red response with decreasing temperature.

The abrupt, additional loss in short circuit current with decreasing temperature, shown by some cells, may be caused by a loss in diffusion length or some other type of collection loss. Cells which showed this abrupt loss in current also had a flat spot on the I-V curve which appeared at the same temperature at which the additional loss in short circuit current began (~ 180°K).

---

(7) G. G. Macfarlane, T. P. McLean, J. E. Quarrington, and V. Roberts, "Fine Structure in the Absorption-Edge of Si," Phys. Rev., Vol. III, pp. 1245-1254; 1958.

(8) M. Wolf, "Drift Fields in Photovoltaic Solar Energy Converter Cells," Proc. IEEE, Vol. 51, pp. 674-693; 1963.

(9) Private communication with Patricia Payne, Heliotek, Division of Textron, Inc., Sylmar, California.

TABLE 1

COMPARISONS BETWEEN PERFORMANCE CURVES AND

CURRENT-VOLTAGE CURVES AT LOW TEMPERATURES

Cell Number	Efficiency under near Jupiter conditions (140°K, 4.6 mw/cm^2)	Performance Curves			Current-Voltage Curves		
		Drop in V_{OC} as temperature decreases	Abrupt drop in I_{SC} as temperature decreases	Drop in P_{MAX} as temperature	Flat spot around P_{MAX}	High series resistance	V_{OC} decreasing with increasing intensity or a curvature near V_{OC}
IP6	15.3					√	√
C191	15.6						√
C206	9.1	√	√	√	√		
C214	14.0	√	√	√		√	√

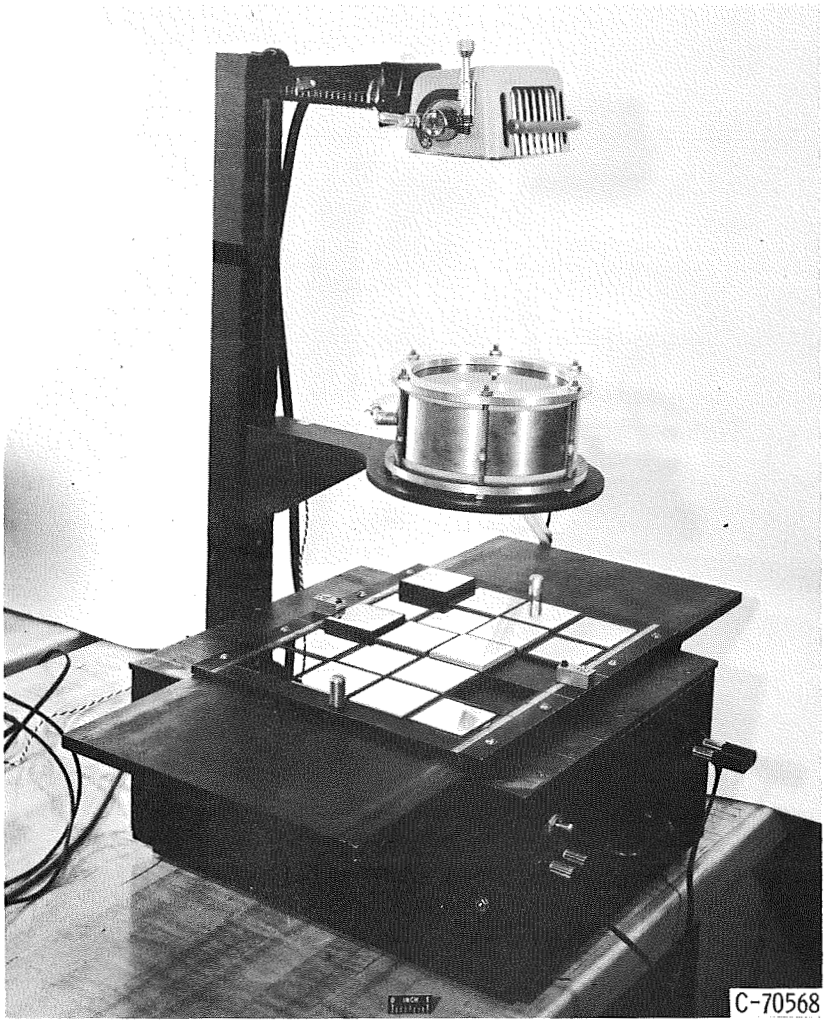

Figure 1. - Apparatus for measuring spectral response.

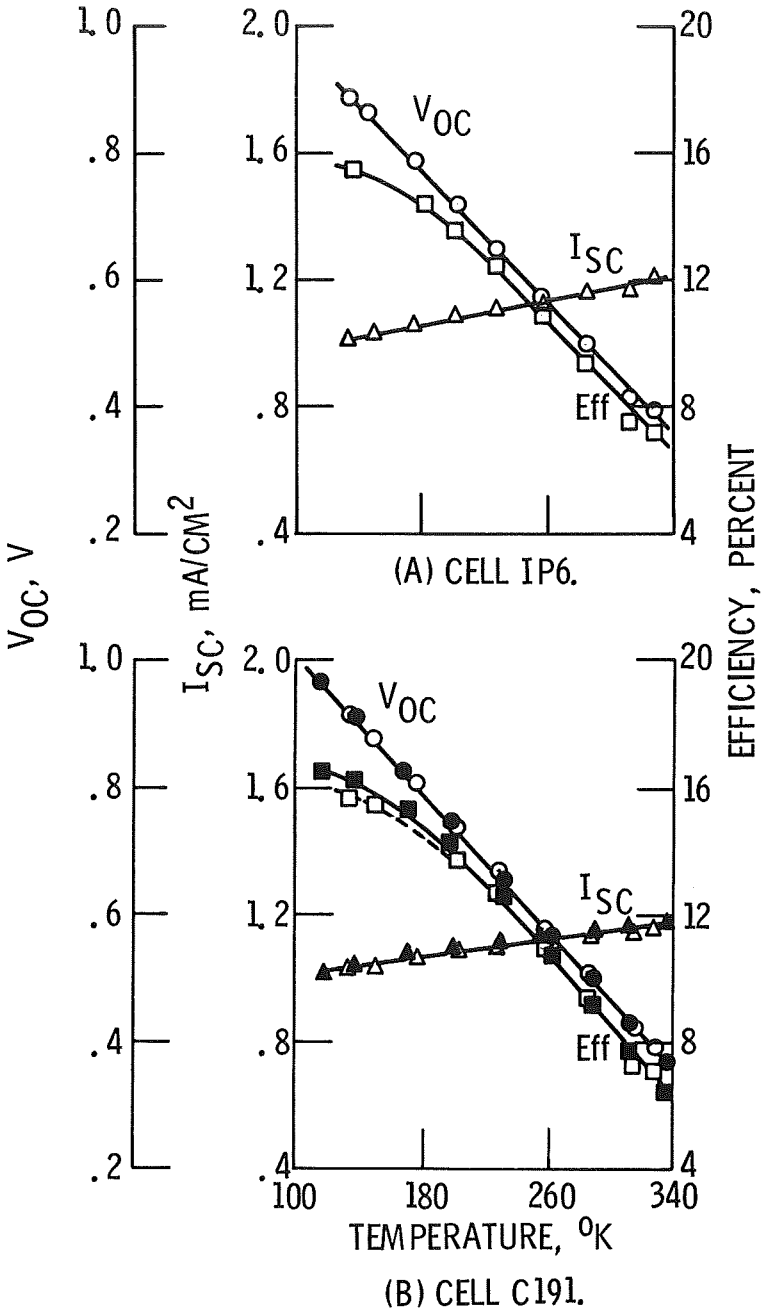

Figure 2. - Performance curves of cells IP6 and C191 as functions of temperature at 4.6 mW/cm^2. Solid data points measured after remounting of cells.

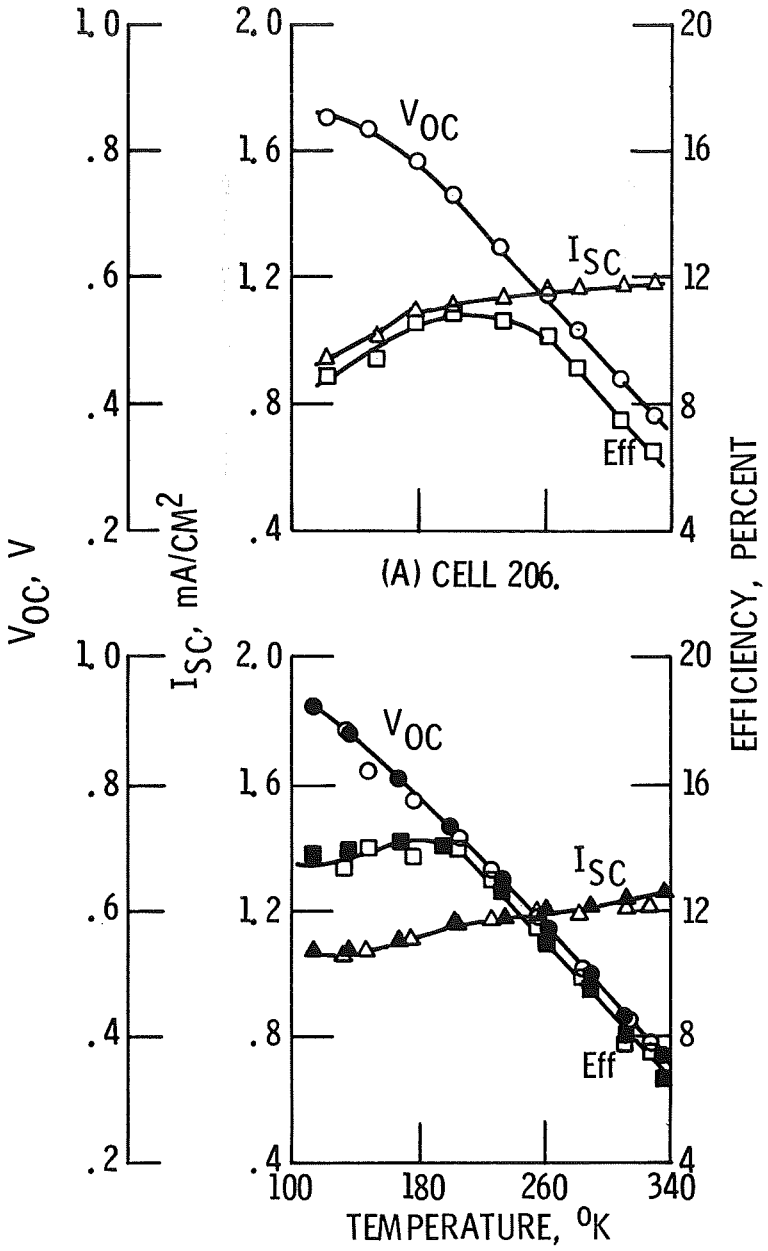

Figure 3. - Performance curves of cells C206 and C214 as functions of temperature at 4.6 mW/cm^2. Solid data points measured after remounting of cells.

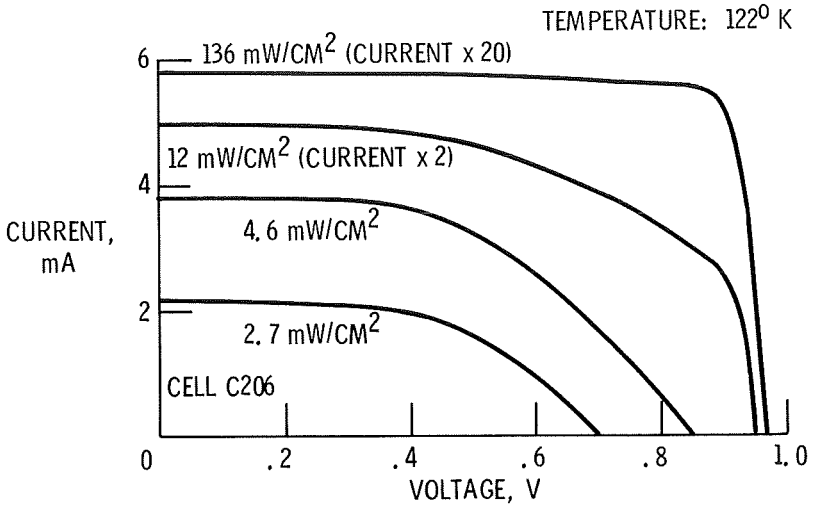

Figure 4. - Current-voltage characteristics of cell C206 at different light levels.

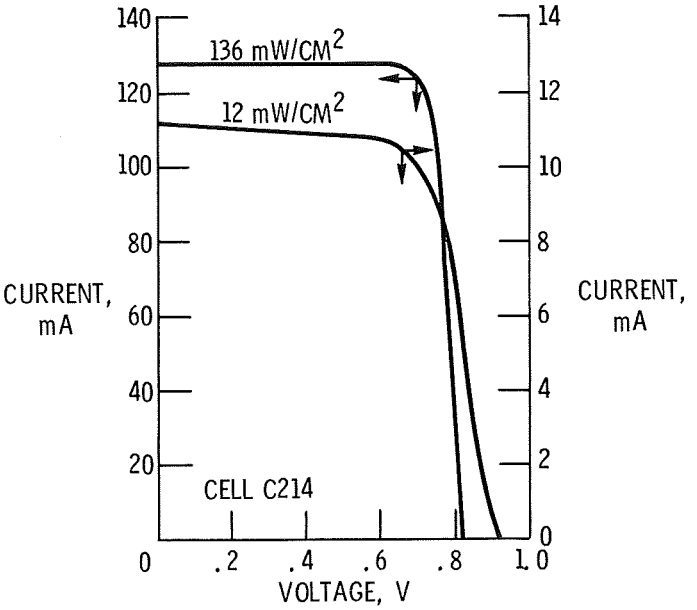

Figure 5. - Current-voltage curve of cell C214 at 114° K at 136 and 12 mW/cm^2.

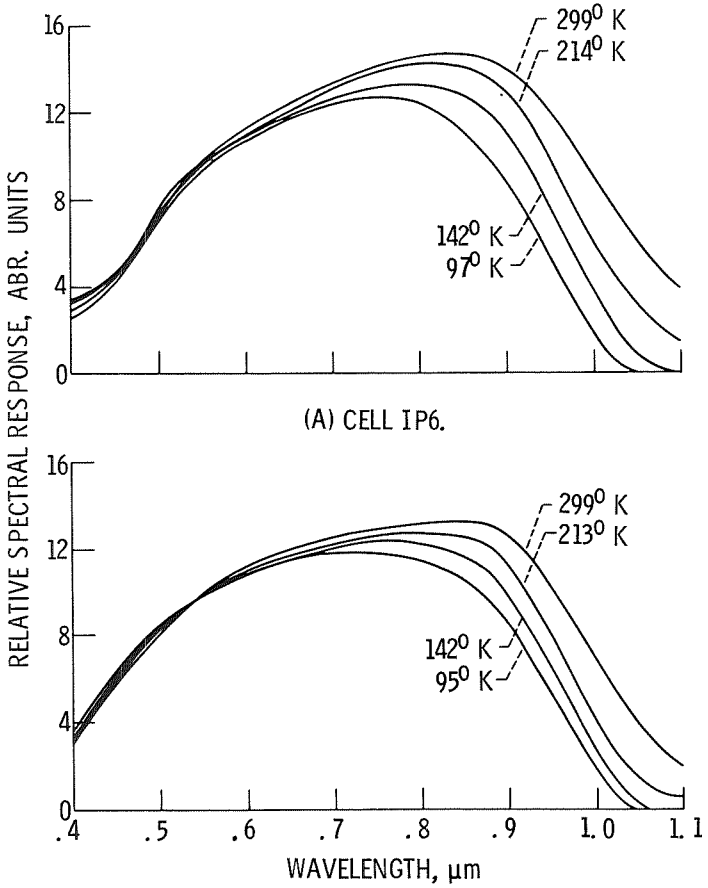

Figure 6. - Relative spectral response of cells IP6 and C191.

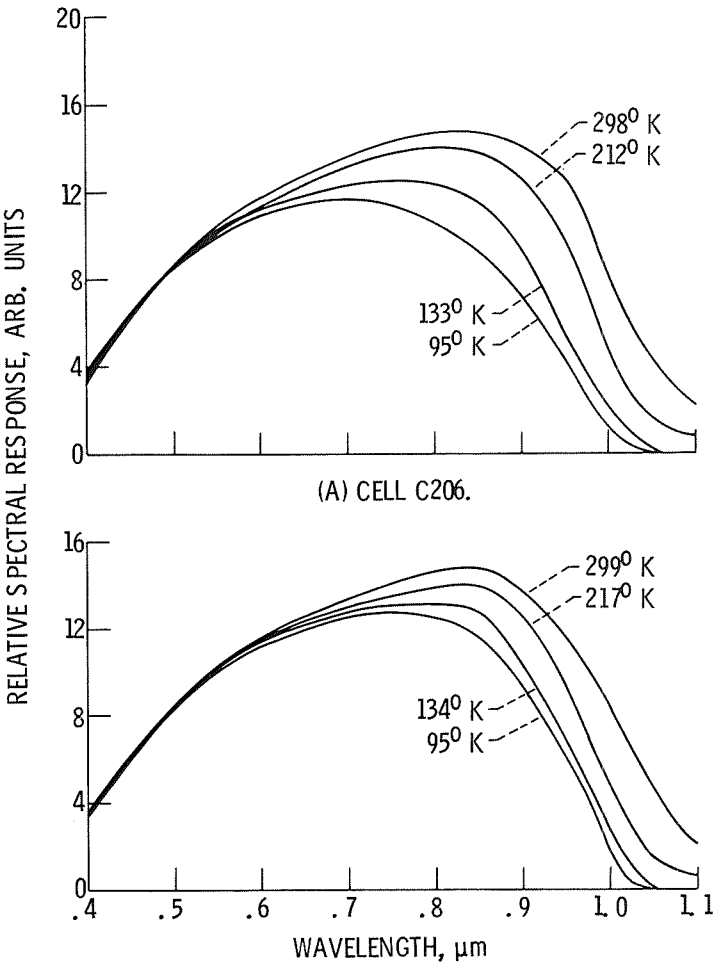

Figure 7. - Relative spectral response of cells C206 and C214.

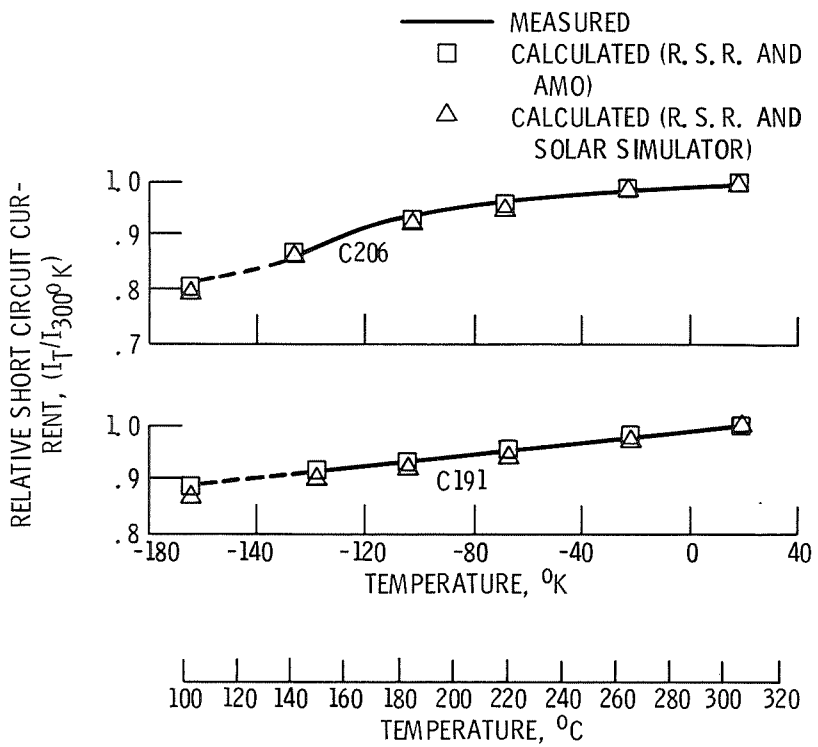

Figure 8. - Comparison between observed and calculated short circuit current temperature dependence. Calculated values obtained by multiplying relative spectral response (RSR) by AMO spectrum and by solar simulator spectrum.

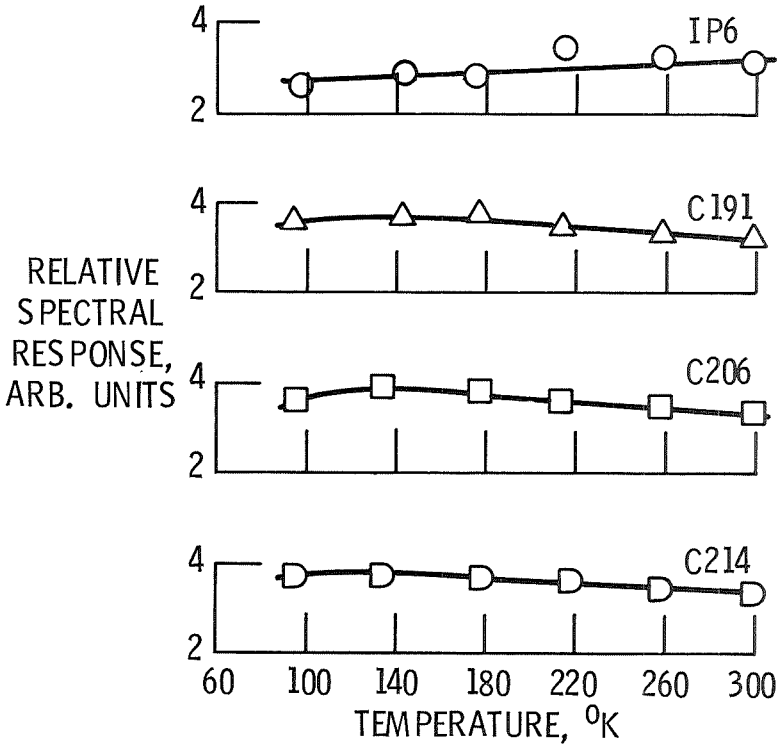

Figure 9. - Temperature dependence of response of silicon solar cells to 0.4 μm light.

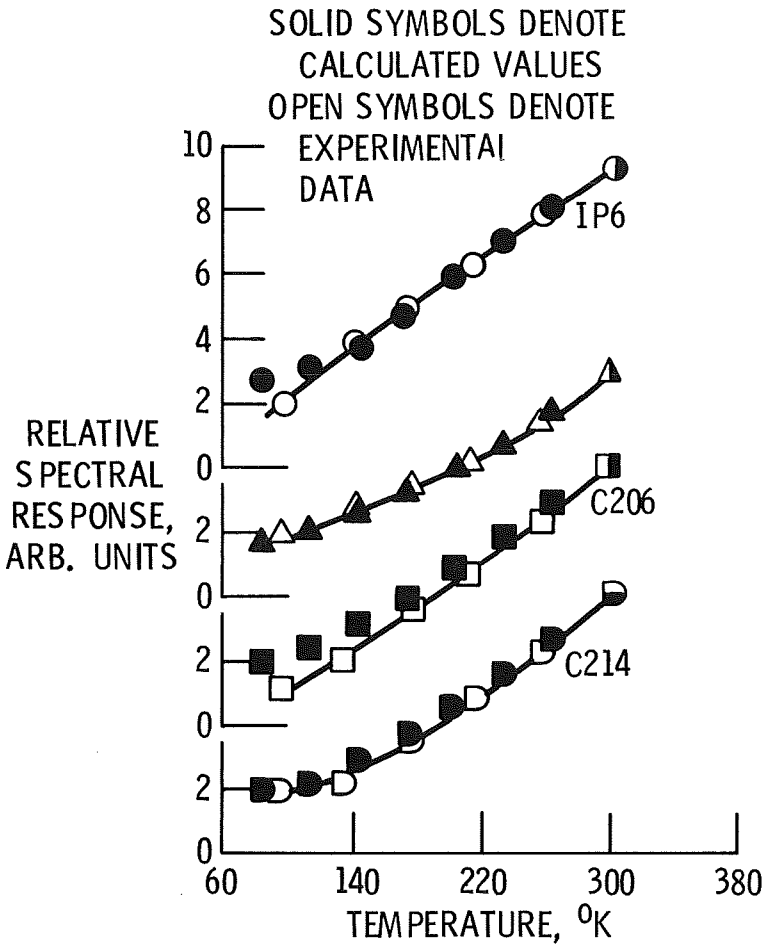

Figure 10. - Temperature dependence of response of silicon solar cells to 1.0 μm light.